Arabian Journal of Chemistry (2020) 13, 4170–4179

King Saud University

Arabian Journal of Chemistry

www.ksu.edu.sa
www.sciencedirect.com

ORIGINAL ARTICLE

Optimization study by Box-Behnken design (BBD) and mechanistic insight of CO_2 methanation over Ru-Fe-Ce/γ-Al_2O_3 catalyst by in-situ FTIR technique

Malik Muhammad Asif Iqbal [a], Wan Azelee Wan Abu Bakar [a,*], Susilawati Toemen [a], Fazira Ilyana Abdul Razak [a], Nur Izyan Wan Azelee [b]

[a] *Department of Chemistry, Faculty of Science, Universiti Teknologi Malaysia, 81310 UTM Johor Bahru, Johor, Malaysia*
[b] *School of Chemical and Energy Engineering, Faculty of Engineering, Universiti Teknologi Malaysia, 81310 UTM Johor Bahru, Johor, Malaysia*

Received 7 May 2019; accepted 17 June 2019
Available online 22 June 2019

KEYWORDS

Carbon dioxide;
BBD;
FTIR

Abstract The utilization of carbon dioxide for methanization reactions in the production of synthetic natural gas (SNG) is of increasing interest in energy-related issues. The use of CO_2 as a raw material in methanization reactions in the formation of SNG is of increasing concern associated with energy problems. The effect of three independent process parameters (calcination temperature, ceria loading and catalyst dosage) and their interactions in terms of conversion of CO_2 was considered by response surface methodology (RSM). Box-Behnken design (BBD) revealed that the optimized parameters were 1000 °C calcination temperature, 85%wt ceria loading and 10 g catalyst dosage, which resulted in 100% conversion of CO_2 and 93.5% of CH_4 formation. Reaction intermediate study by in situ FTIR showed that carboxylate species was the most active species on the catalyst surface. In-situ FTIR experiments revealed a weak CO_2 adsorption, that exist namely as carboxylate species over the trimetallic catalyst. As a result, dissociated hydrogen over ruthenium reacts with surface carbon, leading to *CH, which subsequently hydrogenated to produce *CH_2, *CH_3 and finally to the desired product methane. The use of in situ-FTIR study indicated that the CO_2 methanation mechanism does not involve CO as a reaction intermediate. The more detailed mechanism of CO_2 methanation pathways involved over Ru-Fe-Ce/γ-Al_2O_3 catalyst is discussed in

* Corresponding author.
E-mail address: wazelee@kimia.fs.utm.my (W.A.W.A. Bakar).
Peer review under responsibility of King Saud University.

Production and hosting by Elsevier

https://doi.org/10.1016/j.arabjc.2019.06.010

accordance with IR-spectroscopic data. The better catalytic activity and stability over Ru-Fe-Ce (5:10:85)/γ-Al_2O_3 catalyst calcined at 1000 °C showed the presence of moderate basic sites for CO_2 adsorption.

1. Introduction

The catalytic hydrogenation of CO_2 to CH_4, known as the Sabatier reaction, as reported by Sabatier and Senderens in 1902, is a significant catalytic process (Sabatier and Senderens, 1902). The formation of CH_4 from CO_2 hydrogenation occurs in two possible pathways (a) in the process of RWGS shift, the cleavage of C—O bond results in the formation of CH_x species via *HCOH, *H_2CO_2 or *H_3CO intermediates, then CH_x species undergo subsequent hydrogenation reactions to form CH_4. Detailed studies of CO_2 methanation reaction by Xu et al. (2016) revealed that the formation of CH_4 was not seen until the appearance of formate species. They suggested that formate possibly may be a critical intermediate of the methanation reaction. Their point of view was supported by several other groups (Kustov and Tarasov, 2014; Schild et al., 1991; Wang et al., 2015). (ii) In direct cleavage of the C—O bond, the formation of CH_4 occurs via *CO_2 dissociates and forms *CO and *O on various noble metal-based catalysts. *CO undergoes a dissociation reaction to produce *O and *C, which is then hydrogenated to form CH_4. Research conducted by Karelovic and Ruiz (2013) revealed the following statements. First, CO_{ads} species were observed at lower temperature when RWGS did not exist. Second, CO was not detected even at 200 °C. Third, until the temperature increased to 180 °C, formate was not accompanied by CO_{ads} species. Hence, they concluded that the formate species had little effect on the reaction. Similarly, the H-assisted pathway of CO dissociation over Fe and Co catalysts was proposed by Ojeda et al. (2010). Likewise, Solymosi and Pásztor (1987) conducted a spectroscopic study over supported Rh catalyst. They found that dissociation of CO on Rh may contribute to the formation of H_{ads}. Moreover, various intermediates products were observed for the hydrogenation of CO. Thus, in both pathways, the cleavage of C—O bond in H_xCO species is a very important step, and probably defines the overall selectivity of CH_4 in the CO_2 hydrogenation reaction.

In present work, the main objective of using RSM method was to obtain the best optimal conditions for experimental design. In mechanistic reactions, the interactions of CO_2 at the cerium oxide and iron oxide interface that can tune the reaction mechanisms were studied. Adsorption properties of CO_2 depending on the reaction temperature were studied in IR studies. In addition, the results of the FTIR studies are summarized in terms of the cleavage of the C—O bond, and the formation of the C—H bond, which gives an idea of the activation and conversion of CO_2 to methane. The results are related to promote the direct route of CO_2 reduction of methane.

2. Experimental

2.1. Catalyst synthesis

The Ru/Fe/Ce/γ-Al_2O_3 catalyst was synthesized by incipient wetness impregnation method. A fixed amount of Cerium nitrate [$Ce(NO_3)_3{\cdot}6H_2O$] (Sigma-Aldrich) 5 g, requisite amount of iron nitrate [$Fe(NO_3)_3{\cdot}9H_2O$] (QRëC) and ruthenium chloride [$RuCl_3{\cdot}H_2O$] (Acros Organics) were dissolved in 15 mL distilled water with constant stirring for 30 min. 10 g of γ-Al_2O_3 support was immersed into the catalyst solution for 30 min. Next, the supported catalyst was transferred on glass wool and aged for 24 h at 90 °C. Then, it was calcined at 1000 °C for 5 h at a heating rate of 10 °C min^{-1}.

2.2. Catalytic performance

The FTIR in situ method was used to study the nature of surface species during methanation of CO_2 using Ru/Fe/Ce/γ-Al_2O_3 catalyst. Infrared spectra (64 scans per spectrum, resolution 4 cm^{-1}) were obtained with the help of FTIR (Brand: Nicolet Avatar 670 DGTS spectrometer) as shown in Fig. 1. For this study we used a cell of FTIR spectrometer (Brand: Nicolet Avatar 670 DGTS) equipped with KBr windows. Before the study, the catalyst was reduced in H_2 flow at 300 °C for 1 h, after which it was cooled down to 50 °C and background spectra were produced. Then, the reaction mixture (vol%, CO_2: H_2 = 1:4) was fed and the spectra were obtained again. The gas hourly space velocity (GHSV) was adjusted to 636 mL g^{-1} h^{-1}. The spectra were recorded at intervals of 2–3 min for half an hour until it became constant. The obtained spectra were represented after background correction, and subtraction of CO_2 gaseous spectra.

2.3. Response surface methodology (RSM)

In recent years, response surface methodology (RSM) is the prevailing optimization method in use. It is a set of statistical and mathematical methods beneficial for the development, improvement, and optimization of processes. It explains the impact of independent variables, individually or in combination with each other, on the processes (Toemen et al., 2017; Rosid et al., 2018). This methodology not only analyzes the influence of independent variables, but also creates an empirical model describing the appropriate quantity of process. The experimental setup and statistical study were executed using Design-Expert software (version 7.1.6, stat-ease Inc., Minneapolis, USA). The BBD (Box-Behnken design) three-level, three-factor design was used, comprising of 15 experimental runs. In this study, three variables were included: (X_1) calcination temperature (°C), (X_2) Cerium load wt% and (X_3) catalyst dosage, as shown in Table 1. Each variable varied over three levels of −1, 0, +1. The generalized second-order polynomial model employed in the RSM is presented in Eq. (1):

$$Y = \beta_0 + \sum \beta_i X_i + \sum \beta_{ii} X_i^2 + \sum \beta_{ij} X_i X_j \quad (1)$$

where Y represents the predicted response (i.e. initial capacity and Rate constant), whereas β_o,β_i, β_{ii}, and β_{ij} represent the regression coefficient for the term intercept, linear, square

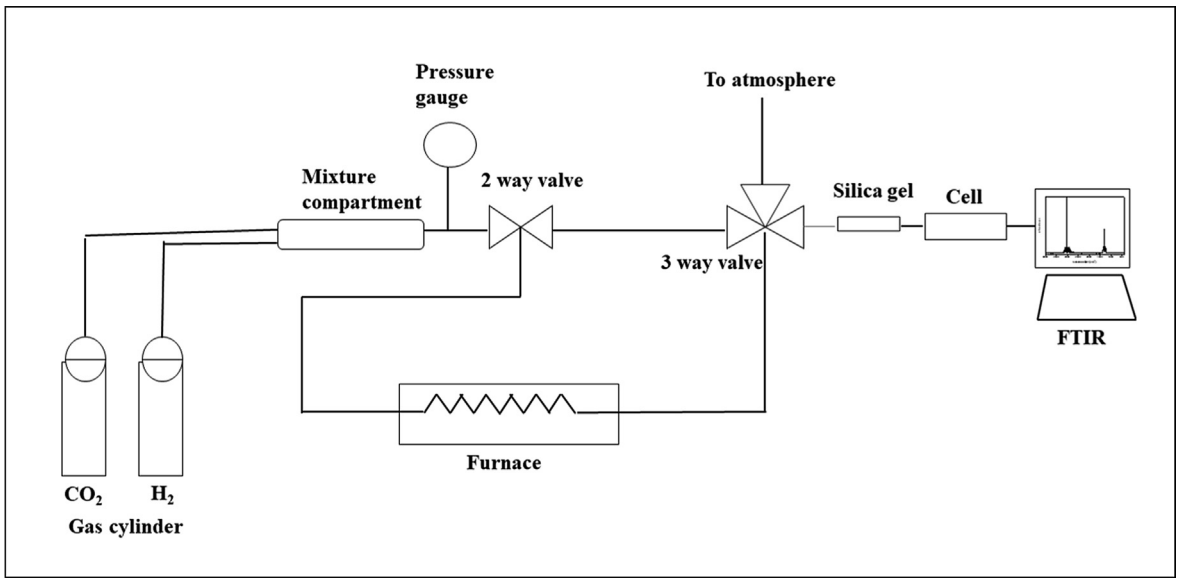

Fig. 1 Systematic diagram of the homebuilt reactor.

and interaction effects, respectively. Also, X_i and X_j are independent variables. The ANOVA table was created, and influence and regression coefficients of individual linear, quadratic and interaction terms were calculated. The values of all second-order polynomial model terms were statistically determined by calculating the F-value.

3. Results and discussion

In this present study, 15 experiments were conducted under the Box-Behnken design (BBD) using Design-Expert software (version 7.1.6, Stat-Ease Inc., Minneapolis, USA) to validate the experimental results.

3.1. Optimization of $Ru/Fe/Ce/\gamma\text{-}Al_2O_3$ by RSM method

In this study, independent variables were: (i) Calcination temperature °C (X_1), (ii) Ce load wt% (X_2) and (iii) catalyst dosage (g) (X_3), as shown in Table 1. The conditions for each process parameter varied at three levels −1, 0, +1.

According to the Box-Behnken design (BBD), experimental design and corresponding results are presented in Table 2. Based on the RSM analysis, the quadratic model for CO_2 conversion is shown the following Eq. (2).

$$Y = 99.35 + 3.52X_1 - 12.60X_2 + 7.62X_3 - 19.83X_1X_2 - 0.54X_1X_3 + 2.12X_2X_3 - 52.92X_1^2 + 13.36X_2^2 - 7.27X_3^2 \quad (2)$$

In this study, the following terms were statistically significant (i) calcination temperature (X_1), (ii) Ce load (X_2), (iii) catalyst dosage (X_3), (iv) calcination temperature^2 (X_1^2), (v) Ce load^2 (X_2^2), (vi) catalyst dosage^2 (X_3^2), and (vii) calcination temperature - Ce load (X_1X_2). Other model terms, including X_1X_3 and X_2X_3 have p-value of 0.1792 and 0.0016, which means that these terms do not have a significant impact on the model. Table 3 shows that the model p-value was lower 0.001, that indicates the high importance of the model. Moreover, Table 3 shows that the F-value is 3338.07 which indicates the high significance of the model. The probability (p-value) of most of the factors and model term is < 0.005. Thus, the model is of great importance, and all three independent variables were considered as model terms.

3.2. Model reliability analysis

A comparison of the actual and predicted CO_2 conversion results for the $Ru/Fe/Ce/\gamma\text{-}Al_2O_3$ catalyst is depicted in Fig. 2.

As can be seen from Fig. 2, there is a very strong convergence between the predicted values and the experimental values for CO_2 conversion. It is noteworthy that Fig. 2 shows both the reliability of the variance analysis and the regression model validity. The high value of $R^2 = 0.9998$ from Table 4, which means high accuracy and good suitability of the model.

Table 4 shows that the value of Pred-$R^2 = 0.9983$ logically coincides with adj-$R^2 = 0.9995$, and also difference is 0.0015, indicating the adequacy of the model applied (Huang et al., 2014). Moreover, the low value of co-efficient of variation

Table 1 Box-Behnken design experiment design and factors.

Process variables	Code	Level Range		
		−1	0	+1
Calcination temp. (°C)	X_1	900	1000	1100
Loading of Ce (wt%)	X_2	80	85	90
Catalyst dosage (g)	X_3	7	10	13

Table 2 Corresponding experimental design using BBD method and response values.

No		Factor Variables			CO_2 conversion (%)	
Standard	Run	X_1	X_2	X_3	Actual	Predicated
11	1	0	−1	+1	96.37	96.83
10	2	0	+1	−1	56.85	56.39
1	3	−1	−1	0	22.33	22.32
14	4	0	0	0	100	99.35
5	5	−1	0	−1	27.11	27.48
2	6	+1	−1	0	69.11	69.02
12	7	0	+1	+1	75.50	75.87
7	8	−1	0	+1	44.25	43.80
15	9	0	0	0	98.63	99.35
13	10	0	0	0	99.43	99.35
4	11	+1	+1	0	4.16	4.17
3	12	−1	+1	0	36.68	36.77
9	13	0	−1	−1	86.19	85.83
8	14	+1	0	+1	50.15	49.78
6	15	+1	0	−1	35.15	35.60

Table 3 Analysis of variance (ANOVA) results for response surface second-order model for the CO_2 conversion over Ru/Fe/Ce/γ-Al_2O_3 catalyst.

Source	Sum of squares	DF	Mean square	F-Value	p-value
Model	14111.58	9	1567.95	3338.07	< 0.0001[a]
X_1	99.40	1	99.40	211.63	< 0.0001
X_2	1270.33	1	1270.33	2704.45	< 0.0001
X_3	464.67	1	464.67	989.25	< 0.0001
X_1X_2	1572.12	1	1572.12	3346.95	< 0.0001
X_1X_3	1.14	1	1.14	2.44	0.1792[b]
X_2X_3	17.94	1	17.94	38.18	0.0016[b]
X_1^2	10341.55	1	10341.55	22016.48	< 0.0001
X_2^2	659.08	1	659.08	1403.14	< 0.0001
X_3^2	194.90	1	194.90	414.94	< 0.0001
Residual	2.35	5	0.47		
Lack of Fit	1.40	3	0.47	0.99	0.5391[b]
Pure Error	0.95	2	0.47		
Cor Total	14113.93	14			

[a] Significant.
[b] Not significant.

(C.V.% = 1.14) reflects the fact that this model proves high reliability and good fitness.

Table 5 shows the parameters for optimization process variables to achieve maximum CO_2 conversion. The main purpose to choose cerium loading as a crucial parameter in the RSM calculation due to the large capacity for storage and release of oxygen by means of redox process $Ce^{4+} \leftrightarrow Ce^{3+}$, it also enhanced the thermal stability of alumina support and improved the dispersion of noble metals (Kašpar et al., 1999). It is established that the mobility of surface oxygen species in CeO_2 is higher in comparison with other metal oxides (Braja, 2003). Thus, 99.99% of CO_2 conversion was achieved under optimal conditions of calcination temperature of 1004.16 °C at a load of Ce 84.54 wt% and catalyst dosage of 9.80 g, which were determined by RSM for this model. The RSM values were close to the experimental value (99.70%) and therefore confirmed the experimental optimization.

The 3D response surface curves were constructed for the CO_2 conversion model (Fig. 3). The surface plots were constructed as a function of two of the factors. Fig. (3a-c) shows the mutual effects of variables in the CO_2 conversion. The interaction of calcination temperature and Ce load at CO_2 conversion is shown in Fig. 3a. Fig. 3a shows a graph of the dependence between calcination temperature and CO_2 conversion, signifying that the calcination temperature has a significant effect on CO_2 conversion. As the calcination temperature rises from 900 to 1000 °C, CO_2 conversion also increases. Meanwhile, with temperature increases from 1000 to 1100 °C, CO_2 conversion is reduced by sintering effect. Therefore, the catalyst with cerium load (85 wt%) and calcined at 1000 °C had the highest CO_2 conversion values.

Fig. 3b shows that the interactions between calcination temperature and catalyst dosage during CO_2 conversion is significant. Fig. 3b shows that the maximum conversion took place with the catalyst dosage of 10 g. Fig. 3a shows that the increase in calcination temperature after 1000 °C resulted in diminution in CO_2 conversion over the Ru/Fe/Ce/γ-Al_2O_3 catalyst. Fig. 3c illustrates the effect of interaction between cerium

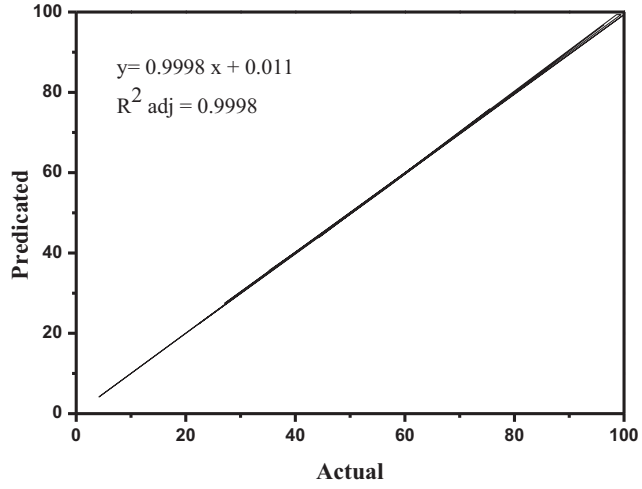

Fig. 2 Comparison of actual and predicted CO_2 conversion results.

Table 4 Model reliability analysis.

Source	Result
Standard deviation	0.69
Mean	60.13
C.V. (%)	1.14
Press	24.55
R^2	0.9998
Adj-R^2	0.9995
Pred-R^2	0.9983
Adeq. precision	170.096

load and catalyst dosage on CO_2 conversion. Hence, the catalyst with 85 wt% cerium load and catalyst dosage (10 g) gave the maximum conversion value of CO_2 (100%) at a reaction temperature of 300 °C.

3.3. Methanation activity

A promising method of obtaining synthetic natural gas is the conversion of CO_2 to CH_4 by methanation reaction. The data of catalytic activity for methanation with FTIR over Ru/Fe/Ce (5:10:85)/γ-Al_2O_3 catalyst at different temperatures were obtained. Before the test, the catalyst was exposed to H_2 atmosphere for 30 min at 300 °C. Then, it was cooled down to room temperature. The values were recorded after 20 min in steady-state conditions for each temperature. The conversion of CO_2 to methane started at around 150 °C, and maximum reaction rate was around 275 °C. The maximum CH_4 production was increased to 93.5% after the reaction temperature was raised to 275 °C. Further increase in temperature, resulting in lower methane production.

The data supporting the suggested view on CO_2 methanation over Ru/Fe/Ce (5:10:85)/γ-Al_2O_3 catalyst were acquired by in situ FTIR spectroscopy. In Fig. 4, the data on CO_2/H_2 (1:4) conversion in contact with Ru/Fe/Ce(5:10:85)/γ-Al_2O_3 at temperatures of 50–300 °C are given. At reaction temperate of 150 °C, only 2.20% of CH_4 is produced over the Ru/Fe/Ce (5:10:85)/γ-Al_2O_3 catalyst, that was calcined at 1000 °C for 5 h. It is noteworthy that the peak relating to CH_4 at 3015.28 cm^{-1} was not detected, as shown in Fig. 4 because it was too small to be noticed. The conversion of CO_2 to methane increases rapidly between temperatures at 200 and 250 °C, while it remains much more stable after reaching a catalyst reaction temperature of 275 °C. Methane selectivity (93.5%) is reduced to 89.8% after reaching the reaction temperature of 280 °C and 92.8% at 290 °C. The results show that at a reaction temperature of 275 °C, a maximum CH_4 production of 93.5% was observed. The selectivity towards methane was achieved 90.88%, whereas a small proportion of 9.12% was detected as a by-product. Hence, at this temperature, intensity peak of CH_4 was appeared and higher occurred.

The FT-IR absorption bands assigned to the vibrational modes ν(C═O) and ν(C─H) species appear at 2358 cm^{-1} and 3016 cm^{-1} respectively. These bands were assigned to monitor the presence of CO_2 and CH_4. Degenerate bending modes of CO_2 starts at a reaction temperature of 150 °C, corresponding to a peak assigned at around 680 cm^{-1}, and intense peak at 2351 cm^{-1}, which corresponds to its asymmetric mode of stretching (Stevens et al., 2008). The weak feature observed between 3600 and 3800 cm^{-1} was attributed to $^{-}$OH stretching mode due to surface water, which is due to the excitation of two modes (Toemen et al., 2017; Jean, 2013). Starting from the reaction temperature of 200 °C, CH_4 was identified in the gas phase, which is characterized by roto-vibrational bands centered at 3016 and 1305 cm^{-1}, attributed to C-H modes of stretching and deformation modes (Nakamoto, 1997). Analysis of the region 2000–1700 cm^{-1} showed that there was no trace of CO species.

3.4. Adsorption studies

Fig. 5 demonstrates the IR-spectra of CO_2 on Ru/Fe/Ce (5:10:85)/γ-Al_2O_3 in CO_2 methanation reactions at 50–300 °C. To further study, the adsorbed species behavior on the surface of the Ru/Fe/Ce(5:10:85)/γ-Al_2O_3 catalyst in the region between 4000 and 450 cm^{-1}, in situ FTIR CO_2 adsorption spectra at different temperatures were recorded. The postulated mechanism of CO_2/H_2 methanation follows the mechanism of Langmuir Hinshelwood, which initially involves the adsorption of CO_2 and H_2 gases on the surface of catalyst (Langmuir, 1918). The analysis of surface species formed on Ru/Fe/Ce(5:10:85)/γ-Al_2O_3 catalyst shows absence of

Table 5 The summarized optimum conditions for RSM model.

	Response	Goal	Lower Limit	Upper Limit	Predicated results	Experiment verified conditions
X_1	Calcination temperature (°C)	In range	900	1100	1004.16	1000
X_2	Ce load (wt%)	In range	80	90	84.54	85
X_3	Catalyst DOSAGE (g)	In range	7	13	9.80	10
Y	Conversion of CO_2 (%)	Target	90	100	99.99	99.70

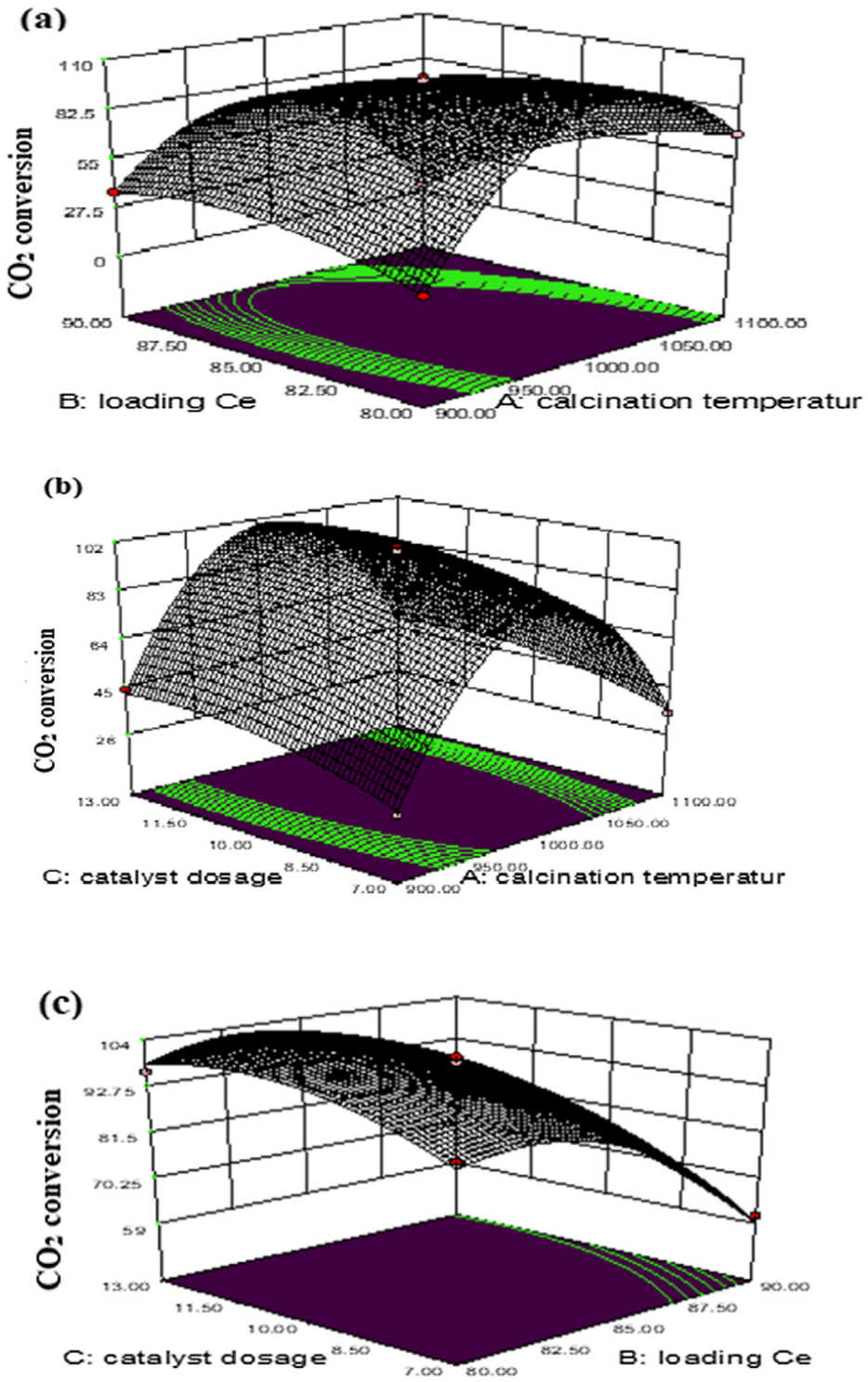

Fig. 3 RSM plots of the combined (a) calcination temperature (°C) vs Ce load (wt%), (b) calcination temperature (°C) vs catalyst dosage (g), and (c) Loading Ce (wt%) vs catalyst dosage (g) on CO_2 conversion.

1504 cm^{-1} (monodentate carbonate), 1567, 1289, 1014, 856 cm^{-1} (bidentate carbonate), 1462, 1351 cm^{-1} (poly dentate carbonates) and 1413, 1218 cm^{-1} (hydrogen carbonate) species (Binet et al., 1999; Yoshikawa et al., 2014). Similarly, the bands assigned to hydrogen carbonates were also absent on the surface of these samples as features at 3616, 1594, 1220 and 1060 cm^{-1} (Daturi et al., 2000). The bands assigned to 1790, 1735, 1218–1087 cm^{-1} (formate species) are also absent (Pan et al., 2014; Li and Domen, 1990).

The deformation band due to hydroxyl group (–OH) at (1640 cm^{-1}) begin to form at 100 °C, it further increases in intensity to a reaction temperature of 290 °C. The adsorbed

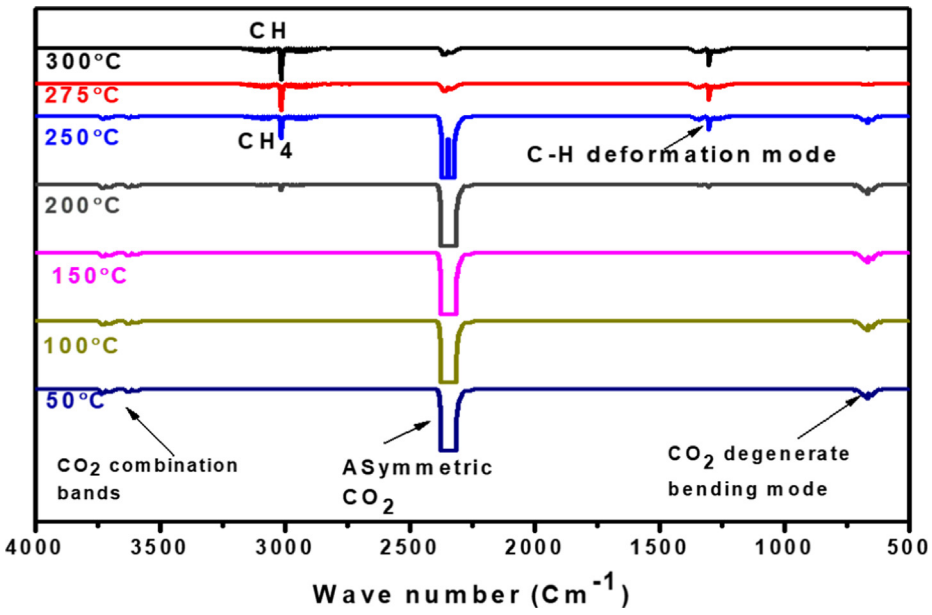

Fig. 4 FTIR spectra of gaseous phases at different reaction temperatures of CO_2/H_2 methanation reaction over Ru/Fe/Ce (5:10:85)/γ-Al_2O_3 catalyst calcined at 1000° C for 5 h.

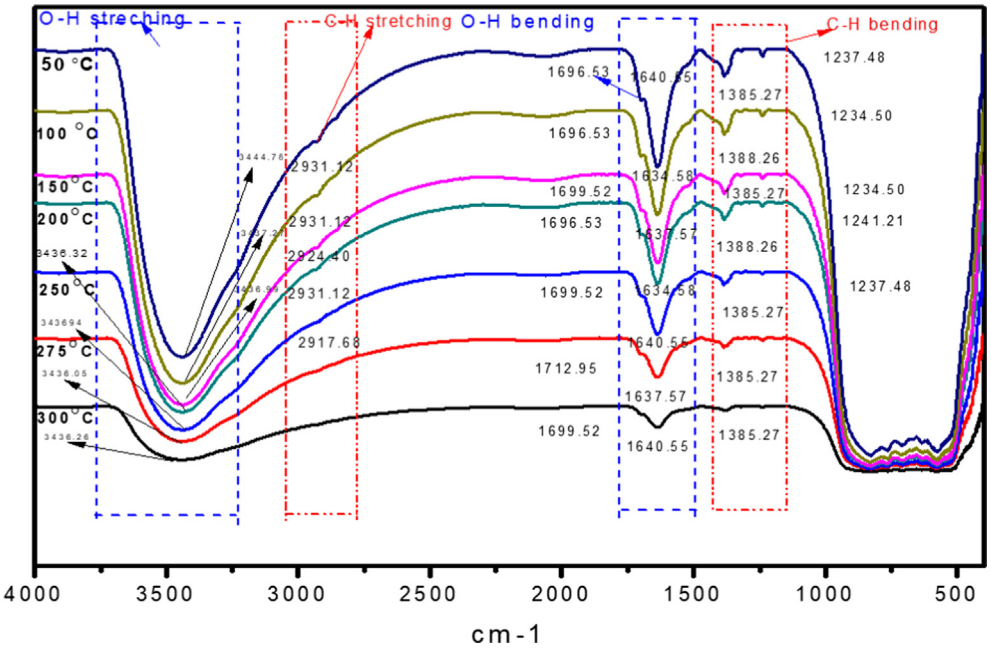

Fig. 5 FTIR spectra of adsorption species on Ru/Fe/Ce (5:10:85)/γ-Al_2O_3 surface at different reaction temperatures calcined at 1000 °C for 5 h.

water has similar properties. The sites for the formation of surface Ce carboxylate group is available during the reaction at reaction temperature of 100 °C. This data indicates that carboxylate specie is formed on the Ru/Fe/Ce(5:10:85)/γ-Al_2O_3 catalyst surface, when a mixture of CO_2/H_2 (1:4) is contacted on catalyst surface during methanation reaction. The catalyst Ru/Fe/Ce (5:10:85)/γ-Al_2O_3 showed two broad O-H regions at 3434 and 1635 cm^{-1}, that were assigned to stretching and bending vibration of adsorbed water on γ-Al_2O_3 support (Muñoz-Murillo et al., 2018). The presence of OH groups highlights the participation of OH groups in the reaction of CO_2 methanation (Karelovic and Ruiz, 2013). Both bands did not display significant variations throughout the reaction temperature. When the reaction temperature was 100 °C, a band appeared at 1641 cm^{-1} (—OH) bonding with a shoulder at around 1701 cm^{-1} corresponding to carboxylate species adsorbed on catalyst surface, as represented in Fig. 5. There is no change in the intensity of carboxylate peak. It shows that carboxylate species adsorption on the surface of very fast. The C—H stretching was started at a reaction temperature of

150 °C, at which a small amount of methane was detected at this temperature as shown in Fig. 5. When the temperature increased from 150 to 275 °C, carboxylate species were hydrogenated by dissociation of hydrogen atoms on the surface of Ru to the formation of hydrocarbon, that lead to the formation of hydrocarbons and finally methane. CO_2 methanation does not take place through CO intermediate. This further proves that when the CO species was detected in the mechanistic study in the gaseous study.

3.5. CO_2 dissociative methanation reaction

The mechanism of reaction, that could consider all these observations, is presented in Fig. 6. The interface of the Ru/Fe/Ce (5:10:85)/γ-Al_2O_3 catalyst offers multiple sites for the adsorption of intermediates reaction products. In this study, formation of CH_4 occurs via the direct cleavage of the C—O bond. In the direct cleavage of the C—O bond pathway, $*CO_2$ is subjected to a dissociation reaction to form *C and *O, or *C and $*CO_2$, followed by hydrogenation of *C to *HC, which is subsequently hydrogenated to produce $*CH_2$, $*CH_3$ and finally the desired product $CH_{4(g)}$ (Weatherbee and Bartholomew, 1982).

Step 1: $*CO_2 \rightarrow *CO_2^-$

Step 2: $*CO_2^- \rightarrow *C + *O$

Step 3: $*C + *H \rightarrow *CH$

Step 4: $*O + *H \rightarrow *OH$

Step 5: $*CH + *H \rightarrow *CH_2$

Step 6: $*OH + *H \rightarrow *H_2O$

Step 7: $*CH_2 + *H \rightarrow *CH_3$

Step 8: $*CH_3 + *H \rightarrow CH_{4(gas)}$

* represents adsorbed species.

The proposed pathway for CO_2 activation and methanation on Ru/Fe/Ce (5:10:85)/γ-Al_2O_3 is shown in Fig. 6. For the methanation CO_2 on Ru/Fe/Ce (5:10:85)/γ-Al_2O_3, Ru metal sites facilitates to the dissociation of molecular H_2, and the spillover of H atoms from Ru metal sites to cerium oxide that formed carboxylate on its surface surfaces.

The CO_2 methanation over Ru/Fe/Ce (5:10:85)/γ-Al_2O_3 catalyst proceeds via bending of straight chain CO_2 on Fe (Choe et al., 2001). Adsorption of CO_2 on the CeO_2 and Fe_2O_3 surface and stepwise hydrogenation to methane through carboxylate intermediates by spilling hydrogen from Ru. In sum, it can be assumed that in the process of methanation CO directly dissociated to carbon (C) and O. Then, at the next stage, hydrogenation of C_{ad} occurred. In situ IR method provide direct observation of intermediate products on the catalyst surface.

3.6. Stability test

The Ru/Fe/Ce (5:10:85)/γ-Al_2O_3 catalyst, calcined at 1000 °C, performed with excellent stability. The stability test graph is shown in Fig. 7.

Ru/Fe/Ce (5:10:85)/γ-Al_2O_3 catalyst, calcined at 1000 °C, was subjected to stability testing at 275 °C because of its relatively outstanding catalytic performance in CO_2 methanation. This is illustrated in Fig. 7, the catalyst showed the best stability for CO_2 conversion within 45 h, with little or no significant reduction in CO_2 conversion (more than 90%). The catalyst's high stability can be ascribed to its relatively moderate basicity and homogenous ruthenium distribution on the support. The

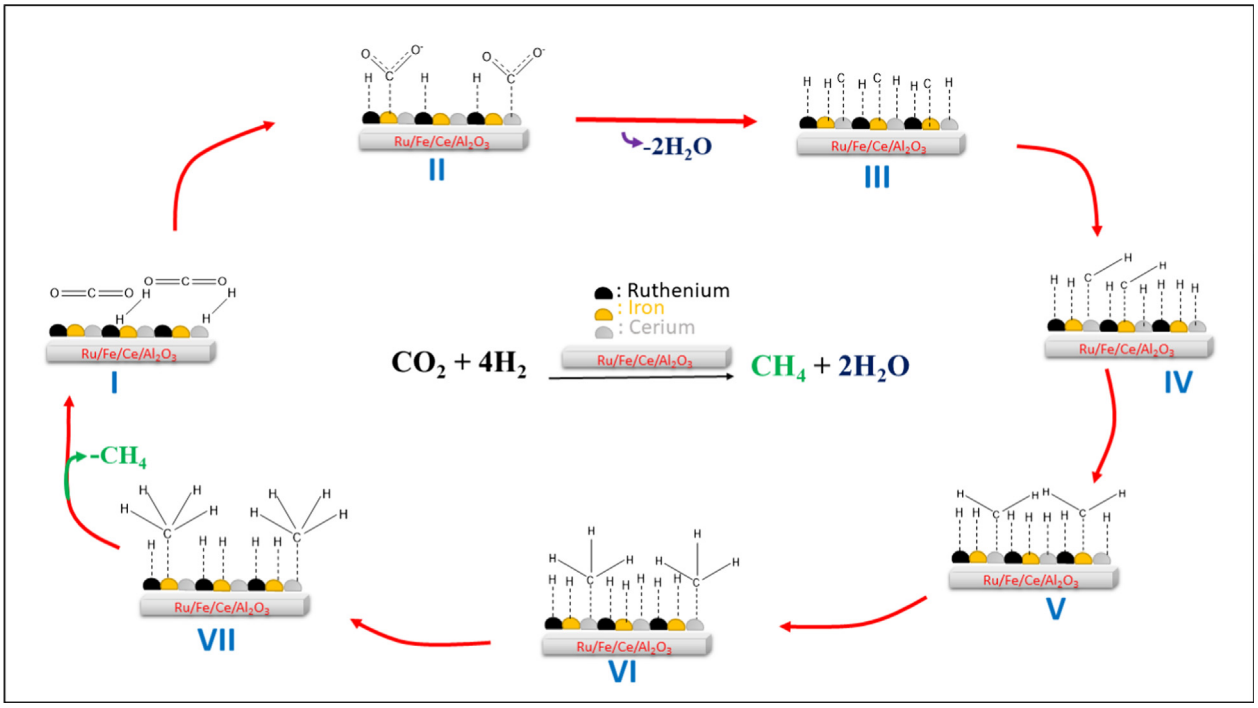

Fig. 6 Proposed reaction pathways for CO_2 methanation on Ru/Fe/Ce (5:10:85)/γ-Al_2O_3 catalyst with plausible intermediates.

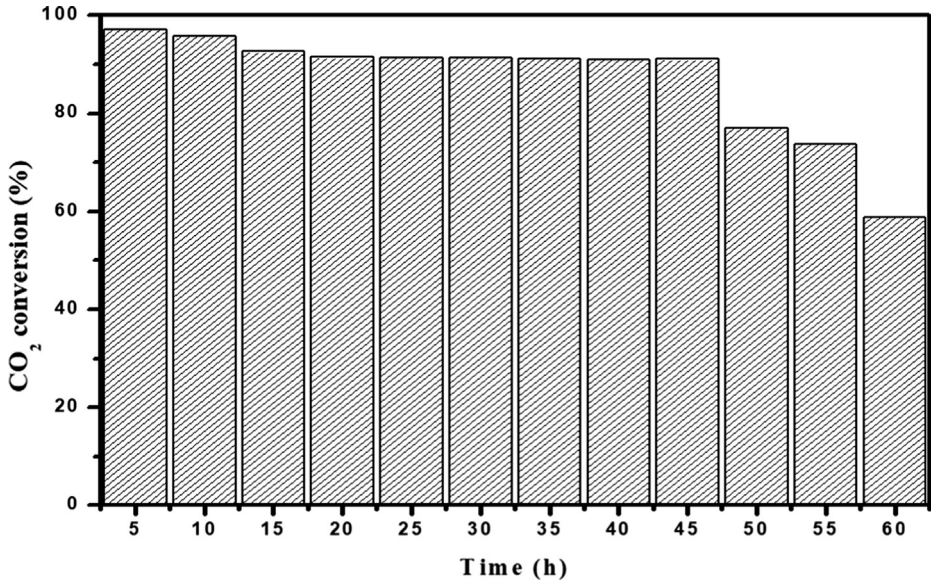

Fig. 7 Stability test result of Ru/Fe/Ce (5:10:85)/γ-Al_2O_3 catalyst calcined at 1000 °C for CO_2 methanation at 275 °C, CO_2/H_2 = 1:4.

Ru/Fe/Ce (5:10:85)/γ-Al_2O_3 catalyst, calcined at 1000 °C, maintains good stability during the experimental period. The results of the catalytic study showed that the Ru/Fe/Ce (5:10:85)/γ-Al_2O_3 catalyst, calcined at 1000 °C, has a high potential for CO_2 methanation due to excellent activity and stability in reaction conditions. The better catalytic performance of Ru/Fe/Ce (5:10:85)/γ-Al_2O_3 catalyst could be attributed to lower iron content that led to the highest selectivity of methane formation (Kang et al., 2011), as compared to our previous work where methane formation was much lower due to high content of iron under similar reaction conditions (Ab Halim et al., 2015), and with similar content of ruthenium (Bakar et al., 2015).

4. Conclusion

The data obtained from in situ FTIR studies have shown that CO_2 methanation occurs on Ru-Fe-Ce/γ-Al_2O_3 catalyst took place via the adsorption of CO_2 on surface of ceria and iron, and then stepwise hydrogenation leads to CH_4 formation through carboxylate intermediate by the hydrogen spilled over from Ru surface.

Acknowledgement

The authors are grateful to acknowledge the Universiti Teknologi Malaysia (UTM) for the financial support provided under Vote no 18H76.

References

Ab Halim, A.Z., Ali, R., Bakar, W.A.W.A., 2015. CO_2/H_2 methanation over M*/Mn/Fe-Al_2O_3 (M*: Pd, Rh, and Ru) catalysts in natural gas; optimization by response surface methodology-central composite design. Clean Technol. Environ. Policy 17 (3), 627–636.

Bakar, W.A.W.A., Ali, R., Mohammad, N.S., 2015. The effect of noble metals on catalytic methanation reaction over supported Mn/Ni oxide based catalysts. Arabian J. Chem. 8 (5), 632–643.

Binet, C., Daturi, M., Lavalley, J.-C., 1999. IR study of polycrystalline ceria properties in oxidised and reduced states. Catal. Today 50 (2), 207–225.

Braja, Gopal M., 2003. Structural, redox and catalytic chemistry of ceria based materials. Bull. Catal. Soc. India 2, 122–134.

Choe, S.J., Kang, H.J., Park, D.H., Park, J., 2001. Adsorption and dissociation reaction of carbon dioxide on Ni (111) surface: molecular orbital study. Appl. Surf. Sci. 181 (3–4), 265–276.

Daturi, M., Binet, C., Lavalley, J., Blanchard, G., 2000. Surface FTIR investigations on $Ce_xZr_{1-x}O_2$ system. Surf. Interface Anal.: Int. J. Dev. Appl. Tech. Anal. Surf., Interfaces Thin Films 30 (1), 273–277.

Huang, Y., Yuan, Y., Zhou, Z., Liang, J., Chen, Z., Li, G., 2014. Optimization and evaluation of chelerythrine nanoparticles composed of magnetic multiwalled carbon nanotubes by response surface methodology. Appl. Surf. Sci. 292, 378–386.

Jean, M.S., 2013. Introduction to molecular vibration and infrared spectroscopy. Chemistry 362, 1–9.

Kang, S.-H., Ryu, J.-H., Kim, J.-H., Seo, S.-J., Yoo, Y.-D., Prasad, P. S.S., et al, 2011. Co-methanation of CO and CO_2 on the Ni_X-Fe_{1-X}/Al_2O_3 catalysts; effect of Fe contents. Korean J. Chem. Eng. 28 (12), 2282–2286.

Karelovic, A., Ruiz, P., 2013. Mechanistic study of low temperature CO_2 methanation over Rh/TiO_2 catalysts. J. Catal. 301, 141–153.

Kašpar, J., Fornasiero, P., Graziani, M., 1999. Use of CeO_2-based oxides in the three-way catalysis. Catal. Today 50 (2), 285–298.

Kustov, L.M., Tarasov, A.L., 2014. Hydrogenation of carbon dioxide: a comparison of different types of active catalysts. Mendeleev Commun. 24 (6), 349–350.

Langmuir, I., 1918. The adsorption of gases on plane surfaces of glass, mica and platinum. J. Am. Chem. Soc. 40 (9), 1361–1403.

Li, C., Domen, K., 1990. Maruya K-i, Onishi T. Spectroscopic identification of adsorbed species derived from adsorption and decomposition of formic acid, methanol, and formaldehyde on cerium oxide. J. Catal. 125 (2), 445–455.

Muñoz-Murillo, A., Domínguez, M., Odriozola, J., Centeno, M., 2018. Selective CO methanation with structured RuO_2/Al_2O_3 catalysts. Appl. Catal. B 236, 420–427.

Nakamoto, K., 1997. Infrared and Raman spectra of inorganic and coordination chemistry. Part A: Theory and Applications in Inorganic Chemistry. Wiley, New York.

Ojeda, M., Nabar, R., Nilekar, A.U., Ishikawa, A., Mavrikakis, M., Iglesia, E., 2010. CO activation pathways and the mechanism of Fischer-Tropsch synthesis. J. Catal. 272 (2), 287–297.

Pan, Q., Peng, J., Sun, T., Wang, S., Wang, S., 2014. Insight into the reaction route of CO_2 methanation: Promotion effect of medium basic sites. Catal. Commun. 45, 74–78.

Rosid, S.J.M., Bakar, W.A.W.A., Ali, R., 2018. Characterization and modelling optimization on methanation activity using Box-Behnken design through cerium doped catalysts. J. Cleaner Prod. 170, 278–287.

Sabatier, P., Senderens, J., 1902. New methane synthesis. Compte Rendu Acad. Sci. Paris 134, 514–516.

Schild, C., Wokaun, A., Koeppel, R.A., Baiker, A., 1991. Carbon dioxide hydrogenation over nickel/zirconia catalysts from amorphous precursors: On the mechanism of methane formation. J. Phys. Chem. 95 (16), 6341–6346.

Solymosi, F., Pásztor, M., 1987. Analysis of the IR-spectral behavior of adsorbed CO formed in $H_2 + CO_2$ surface interaction over supported rhodium. J. Catal. 104 (2), 312–322.

Stevens Jr, R.W., Siriwardane, R.V., Logan, J., 2008. In situ Fourier transform infrared (FTIR) investigation of CO_2 adsorption onto zeolite materials. Energy Fuels 22 (5), 3070–3079.

Toemen, S., Bakar, W.A.W.A., Ali, R., 2017. CO_2/H_2 methanation technology of strontia based catalyst: physicochemical and optimisation studies by Box-Behnken design. J. Cleaner Prod. 146, 71–82.

Wang, X., Shi, H., Kwak, J.H., Szanyi, J., 2015. Mechanism of CO_2 hydrogenation on Pd/Al_2O_3 catalysts: kinetics and transient DRIFTS-MS studies. ACS Catal. 5 (11), 6337–6349.

Weatherbee, G.D., Bartholomew, C.H., 1982. Hydrogenation of CO_2 on group VIII metals: II. Kinetics and mechanism of CO_2 hydrogenation on nickel. J. Catal. 77 (2), 460–472.

Xu, J., Su, X., Duan, H., Hou, B., Lin, Q., Liu, X., et al, 2016. Influence of pretreatment temperature on catalytic performance of rutile TiO_2-supported ruthenium catalyst in CO_2 methanation. J. Catal. 333, 227–237.

Yoshikawa, K., Sato, H., Kaneeda, M., Kondo, J.N., 2014. Synthesis and analysis of CO_2 adsorbents based on cerium oxide. J. CO_2 Util. 8, 34–38.